

Braids of entangled particle trajectories

Jean-Luc Thiffeault*

Department of Mathematics, University of Wisconsin, Madison, WI 53706, USA

(Dated: November 7, 2018)

In many applications, the two-dimensional trajectories of fluid particles are available, but little is known about the underlying flow. Oceanic floats are a clear example. To extract quantitative information from such data, one can measure single-particle dispersion coefficients, but this only uses one trajectory at a time, so much of the information on relative motion is lost. In some circumstances the trajectories happen to remain close long enough to measure finite-time Lyapunov exponents, but this is rare. We propose to use tools from braid theory and the topology of surface mappings to approximate the topological entropy of the underlying flow. The procedure uses all the trajectory data and is inherently global. The topological entropy is a measure of the entanglement of the trajectories, and converges to zero if they are not entangled in a complex manner (for instance, if the trajectories are all in a large vortex). We illustrate the techniques on some simple dynamical systems and on float data from the Labrador sea. The method could eventually be used to identify Lagrangian coherent structures present in the flow.

Keywords: topological chaos, dynamical systems, Lagrangian coherent structures

Consider particles floating on top of a fluid. We can follow their trajectories, either with a camera or by computer simulation. If we then plot their position in a three-dimensional graph, with time the vertical coordinate, we get a ‘spaghetti plot,’ which contains information about how entangled the trajectories are. We discuss how to measure the level of entanglements in terms of topological entropy, and the interpretation of the results. This provides a straightforward method of estimating the level of chaos present in a system. This approach could also be used to determine if some trajectories remain together for a long time, and are thus part of a Lagrangian coherent structure.

I. INTRODUCTION

A. Floats in the ocean: an example

Figure 1(a) shows the trajectories of ten floats released in the Labrador sea, for a period of a few months. The principal reason to release such floats is the data they measure and transmit back – temperature, salinity, pressure, etc. But the actual trajectories of the floats are also important, since they tell us something about large-scale transport in the ocean, a crucial component in understanding global circulation. From a single float one can deduce the single-particle dispersion coefficient, a crude measure of how quickly a float wanders away from its release point. However, it is better to measure quantities that

*Electronic address: jeanluc@math.wisc.edu

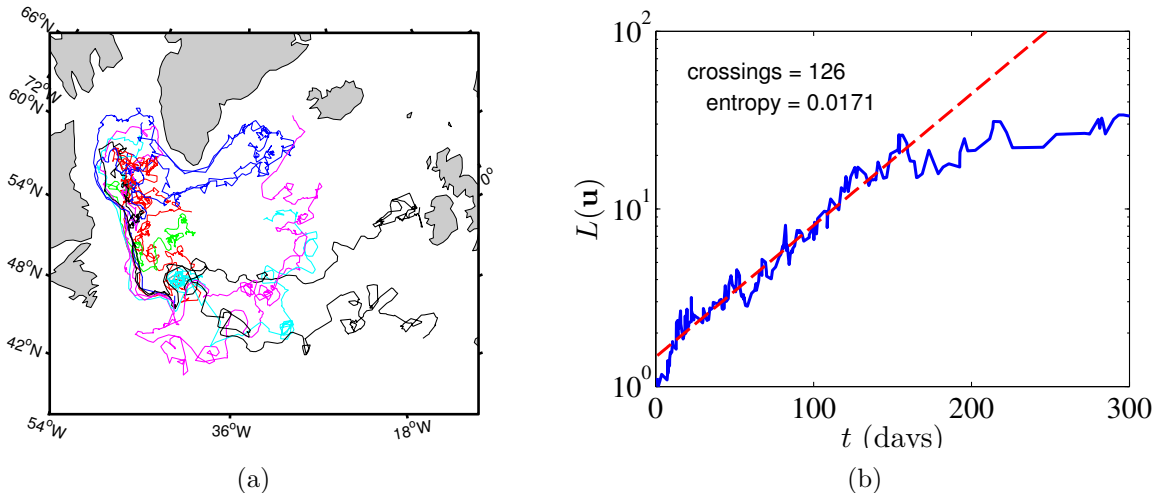


FIG. 1: (a) 10 floats from Davis’ Labrador sea data [1]. (b) The growth of $L(\mathbf{u})$ for the 10 floats, with a fit of the topological entropy. For longer times, the floats leave the Labrador sea and $L(\mathbf{u})$ becomes constant. The details of the analysis are presented in Section IV.

involve several floats [2]. For instance, if floats happen to start near each other, then we can see how quickly they separate and measure finite-time Lyapunov exponents [3], which are linked to chaotic advection [4]. But if the floats are nowhere near each other, then a more global quantity is needed. In this paper we propose to examine the ‘braid’ defined by the trajectories and to measure their degree of entanglement. (All these terms will be defined more precisely.) The number we get out of this is called the braid’s *topological entropy*. Figure 1(b) shows a measure of the entanglement of the ten floats as a function of time, with an exponential fit: the growth rate is the topological entropy. (For longer times, the curve levels off because floats start leaving the Labrador sea, which is not really a closed system.) Much like a Lyapunov exponent, the topological entropy gives us a characteristic time for the entanglement of the floats in the Labrador sea, here about $1/0.02 \simeq 50$ days.

B. Topology and trajectories

Since the original paper of Boyland *et al.* [5], topological techniques in fluid dynamics have been applied to free point vortices [6], fixed blinking vortex [7, 8], rod stirring devices [9, 10, 11, 12, 13], and spatially-periodic systems [14, 15]. (See [16] for a brief review.) More recently, the emphasis has shifted to locating periodic orbits that play an important role in stirring [9, 12] — so-called *ghost rods* — and even to the manufacture of such orbits [17]. Most of these papers study periodic motions of rods or particle orbits. For many practical applications, however, periodic motion is not directly observable, since most such orbits are highly unstable. Hence, some authors have examined *random braids* [7, 14, 16, 18, 19] composed of arbitrary chaotic trajectories. (There is also related literature from the knot theory perspective — see for example [20].)

The goal of the present paper is to give concrete techniques that can be used to obtain topological information from particle trajectories. The mathematical details are glossed over: the emphasis is on usability. Implementation details are discussed, and some sample Matlab

programs are presented in an appendix. The hope is that this will make these techniques more accessible to those with little or no background in braid theory and topology.

The principal measurement we extract from a braid is its topological entropy. This entropy is closely related to the traditional Lyapunov exponent, except that being a topological quantity it is not sensitive to the size of the sets on which chaos is occurring. This is both a weakness and a strength: it does not tell us everything we might like to know, but on the other hand the topological entropy is easy to compute from crude data. This is in contrast to Lyapunov exponents, which require at the very least detailed knowledge of particle trajectories that start close together, and at best the velocity field and its gradient. When dealing with, for example, data from oceanic floats (as we will later in this paper), being able to compute a Lyapunov exponent is a rarity.

There is also a philosophical point that bears some discussion. The viewpoint of the present paper is that given particle trajectory data, a useful thing to quantify is how ‘entangled’ the particle trajectories are. This can be done from the particle data directly, without worrying about the underlying flow. By contrast, Lyapunov exponents are defined locally and are sensitive to the *smooth structure* of the flow. It is exactly the (presumed) smooth nature of the flow that connects local information to a global quantity such as the Lyapunov exponent, but one is left wondering why we should care about the local picture at all in practical situations. The topological viewpoint presented here is an attempt to sidestep this and focus directly on global information.

We begin in Section II by a short introduction to braid theory, surface dynamics, and their connection to dynamical systems. In Section II B we show how to extract braids from particle trajectory data. Section III is devoted to topological entropy: in Section III A we discuss its connection to flows, and in Section III B we show how to measure it from a braid (for a braid corresponding to periodic orbits). In Section IV we introduce random braids, and again show how to measure entropies. As an application, we calculate the entropy for floats in the Labrador sea, as presented in Fig. 1. We offer some concluding remarks in Section V.

II. BRAIDS

A. Physical and Algebraic braids

First we describe intuitively how braids arise. Figure 2(a) shows the orbits of 4 particles in a circular two-dimensional domain. The particles might be fluid elements, solutions of ordinary differential equations, or physical particles at the surface of a fluid. Figure 2(b) shows the ‘world line’ of the same orbits: they are plotted in a three-dimensional graph, with time flowing vertically upwards. The diagram in Fig. 2(b) depicts a *physical braid*, made up of four strands. No strand can go through another strand as a consequence of the deterministic motion of the particles (they never occupy the same point at the same time). Moreover, the mathematical definition of a braid requires that strands cannot ‘loop back’: here this simply means that the particles cannot travel back in time. We will say that two braids are equivalent if they can be deformed into each other with no strand crossing other strands or boundaries. Throughout this paper, we will be interested in characterizing the level of ‘entanglement’ of trajectories.

Since we can move the strands, is convenient to draw braids in a normalized form, as shown in Fig. 2(c) for the braid in Fig. 2(b). Such a picture is called a *braid diagram*. The

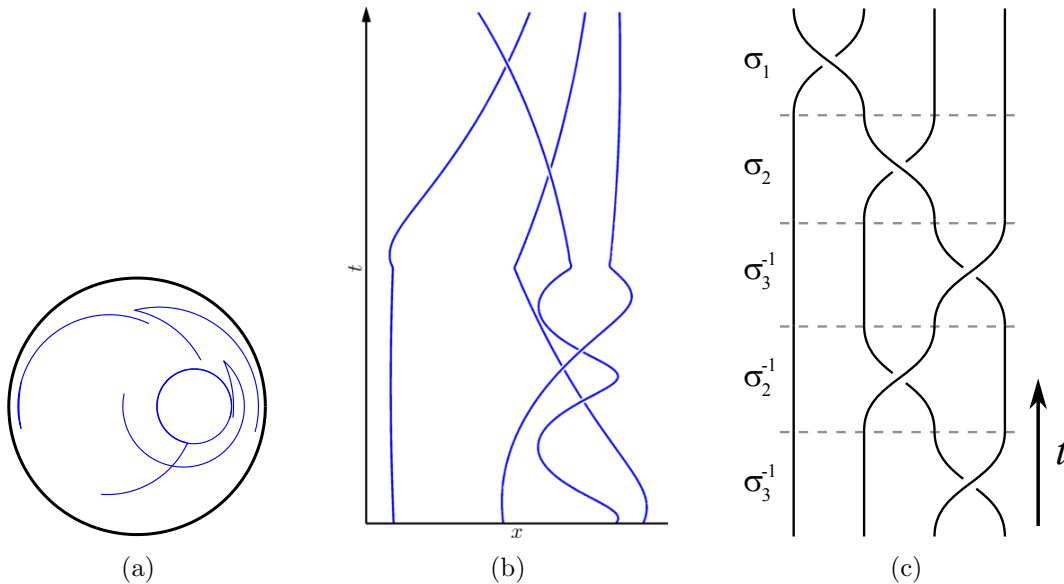


FIG. 2: (a) The orbits of four particles in a circular two-dimensional domain; (b) The same orbits, lifted to a space-time diagram in three dimensions, with time flowing from bottom to top. (c) The standard braid diagram corresponding to (b).

important thing is that we record when crossings occur, and which particle was behind and which was in front. It matters little how we define ‘behind,’ as long as we are consistent (see Section II B for practical considerations). In Fig. 2(c) the horizontal dashed lines also suggest that we can divide the braid into a sequence of elementary crossings, known as *generators*. Figure 3(a) shows the definition of σ_i , which denotes the clockwise interchange of the i th and $(i + 1)$ th strands, keeping all other strands fixed. Note that the index i is the position of the strand from left to right, *not* a label for the particular strand. For n strands, we have $n - 1$ distinct generators.

Figure 3(a) also shows the counterclockwise interchange of two strands, denoted by the operation σ_i^{-1} . The justification of the ‘inverse’ notation is evident in Fig. 3(b): if we concatenate σ_i and σ_i^{-1} , then after pulling tight on the strands we find that they are disentangled. We call the braid on the right in Fig. 3(b) the *identity braid*. In fact, the set of all braids on a given number n of strands forms a *group* in the mathematical sense: the group operation is given by concatenation of strands, the inverse by reversing the order and direction of crossings, the identity is as described above, and it is clear that concatenation is associative. This group is called B_n , the braid group on n strands, also known as the Artin braid group.

The braid group B_n is generated by the set $\{\sigma_1, \dots, \sigma_{n-1}\}$: this means that any braid in B_n can be written as a product (concatenation) of σ_i ’s and their inverses. The braid group is *finitely-generated*, even though it is itself infinite: only a finite number of generators give the whole group. To see that the braid group contains an infinite number of braids, simply consider σ_1^k , for k an arbitrary integer: no matter how large k gets, we always get a new braid out of this, consisting of increasingly twisted first and second strands.

We have now passed from physical braids, as depicted in Fig. 2(b), to *algebraic braids*. The algebraic braid corresponding to Fig. 2(c) is $\sigma_3^{-1}\sigma_2^{-1}\sigma_3^{-1}\sigma_2\sigma_1$, where we read generators

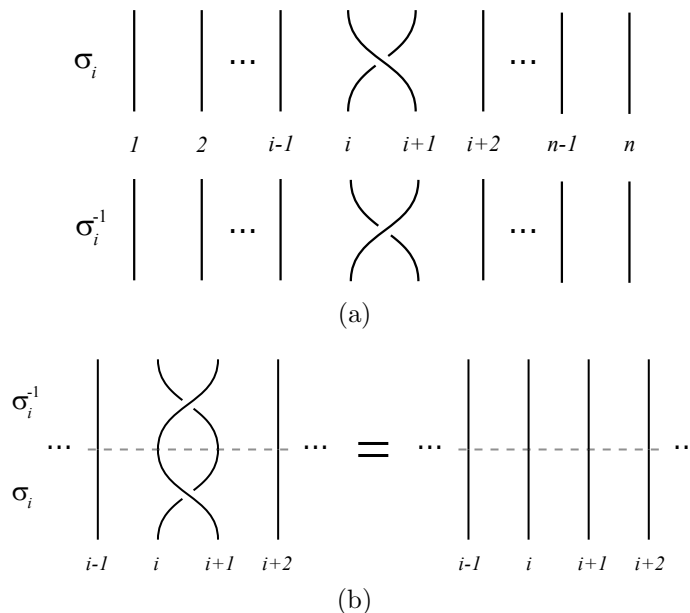


FIG. 3: (a) Braid group generator σ_i , corresponding to the clockwise interchange of the string at the i th and $(i + 1)$ th position, counted from left to right. Its inverse σ_i^{-1} involves their counter-clockwise exchange. (b) The concatenation of σ_i and σ_i^{-1} gives the identity braid.

from left to right in time (beware: conventions differ). In essence, an algebraic braid is simply a sequence of generators, which may or may not come from a physical braid. How can we guarantee that physical braids and algebraic braids describe the same group? We need to be mindful of *relations* amongst the generators that arise because of physical constraints. For example, Fig. 4(a) shows a relation amongst adjacent triplets of strands. Staring at the picture long enough, and allowing for the deformation of strands without crossing, the reader can perhaps see that braids in Fig. 4(a) are indeed equal. Hence, the algebraic sequence $\sigma_i\sigma_{i+1}\sigma_i$ must be equal to $\sigma_{i+1}\sigma_i\sigma_{i+1}$, if the generators are to correspond to physical braids. Another, more intuitive relation is shown in Fig. 4(b): generators commute if they do not share a strand. In summary, we have the relations

$$\sigma_i\sigma_j\sigma_i = \sigma_j\sigma_i\sigma_j \quad \text{if } |i - j| = 1, \quad (1a)$$

$$\sigma_i\sigma_j = \sigma_j\sigma_i \quad \text{if } |i - j| > 1, \quad (1b)$$

amongst the generators. Artin [21] proved the surprising fact that there are no other relations satisfied by the generators σ_i , except for those that can be derived from (1) by basic group operations (multiplication, inversion, etc.). The generators $\{\sigma_1, \dots, \sigma_{n-1}\}$ together with the relations (1) define the *algebraic braid group*, which we also denote B_n . With these relations, the groups of physical and algebraic braids are isomorphic.

A consequence of the relations (1) is that it may not be immediately obvious that two algebraic braids are equal. For instance, the braids $\sigma_1\sigma_2$ and $\sigma_2\sigma_2\sigma_1\sigma_2\sigma_1^{-1}\sigma_1^{-1}$ are equal, since

$$\sigma_1\sigma_2 = (\sigma_1\sigma_2\sigma_1)\sigma_1^{-1} = (\sigma_2\sigma_1\sigma_2)\sigma_1^{-1} = \sigma_2(\sigma_1\sigma_2\sigma_1)\sigma_1^{-1}\sigma_1^{-1} = \sigma_2\sigma_2\sigma_1\sigma_2\sigma_1^{-1}\sigma_1^{-1}.$$

This ‘braid equality’ problem has seen many refinements: the original solution of Artin [21]

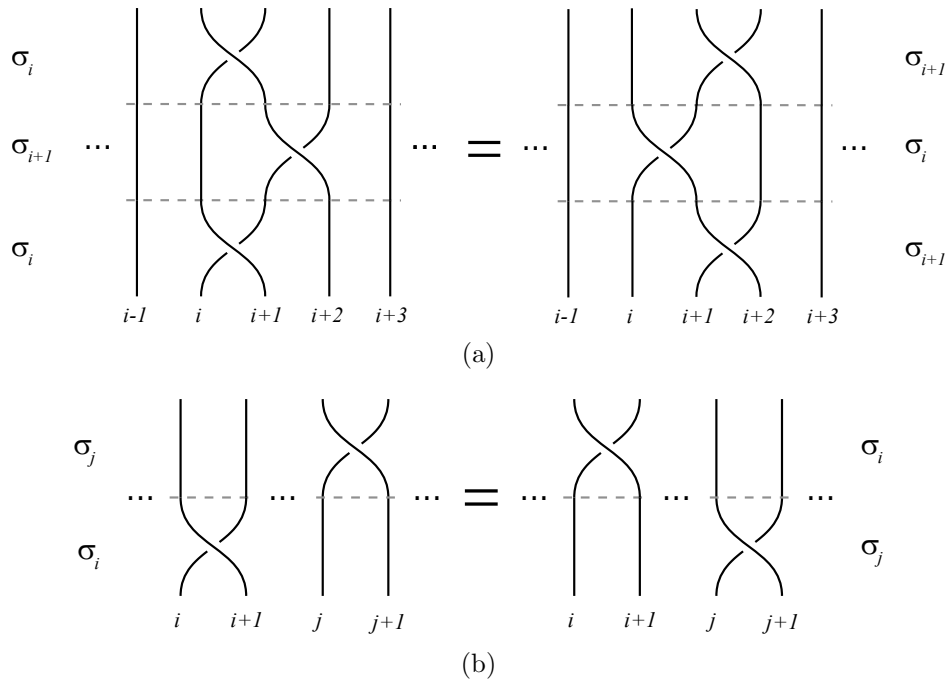


FIG. 4: Braid group relations (see Eq. (1)): (a) relation for three adjacent strands; (b) commutation relation for generators that don't share a strand.

has computational complexity exponential in the number of generators, but modern techniques can determine equality in a time quadratic in the braid length [22, 23, 24].

B. Extracting the braid from a flow

The first step in obtaining useful topological information from particle trajectories is to compute their associated braid, essentially going from the physical picture in Fig. 2(b) to the algebraic picture in Fig. 2(c). A simple method to do this was originally described in [7], but is also implicit in earlier work such as [18, 25] (see also [26] for a related technique).

We start with trajectory information for n particles over some time. We first project the position of the particles onto any fixed *projection line* (which we choose to be the horizontal axis), and label the particles by $i = 1, 2, \dots, n$ in increasing order of their projection. A crossing occurs whenever two particles interchange position on the projection line. A crossing can occur as an “over” or “under” braid, which for us means a clockwise or counterclockwise interchange. These interchanges correspond to the braid group generators introduced in Section II A.

Assuming a crossing has occurred between the i th and $(i + 1)$ th particles, we need to determine if the corresponding braid generator is σ_i or σ_i^{-1} . We look at the projection of the i th and $(i + 1)$ th particles in the direction perpendicular to the projection line (the vertical axis in our case). If the i th particle is *above* the $(i + 1)$ th at the time of crossing, then the interchange involves the group generator σ_i (we define “above” as having a greater value of projection along the perpendicular direction). Conversely, if the i th particle is *below* the $(i + 1)$ th at the time of crossing, then the interchange involves the group generator σ_i^{-1} .

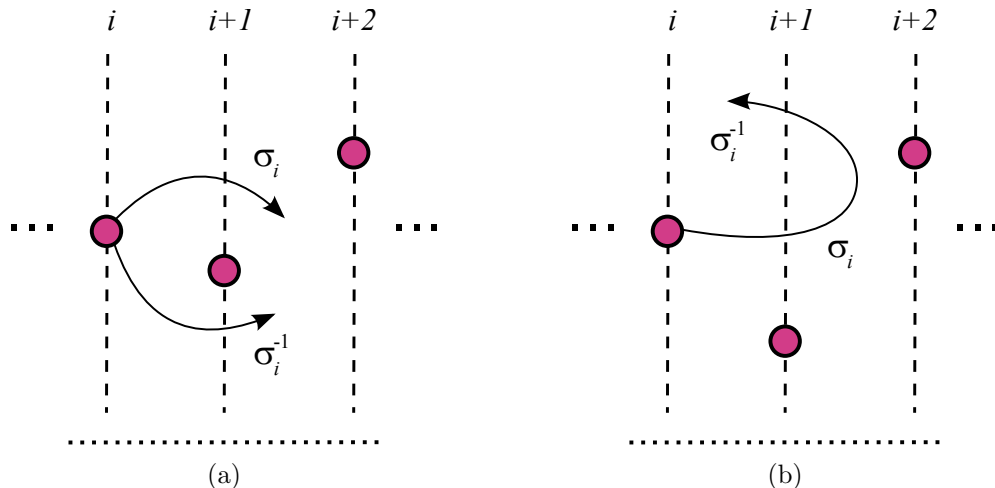


FIG. 5: Detecting crossings: (a) Two possible particle paths that are associated with different braid group generators; (b) Two crossings that yield no net braiding. The projection line used to detect crossings is shown dotted at the bottom, and the perpendicular lines used to determine the braid generator are shown dashed.

Figure 5(a) depicts these two situations.

The net result is that from the n particle trajectories we obtain a time-ordered sequence of the generators σ_i and σ_i^{-1} , $i = 1, \dots, n - 1$. We call this sequence the braid of the trajectories. We also record the times at which crossings occur, so each generator in the sequence has a time associated with it.

Remarks:

- The method just described might seem to detect spurious crossings if two well-separated particles just happen to interchange position on the projection line several consecutive times in a row, as shown in Figure 5(b). However, this would imply a sequence of σ_i and σ_i^{-1} braid generators, since which particle is the i th one changes at each crossing. When composed together the generators for these crossings cancel.
- We give a simple Matlab implementation of the method in Appendix A 1. The program `gencross` detects crossings in trajectory data; it makes an effort to resolve multiple simultaneous crossings (up to triple crossings), but will complain if it gets confused. More sophisticated code can be written that re-interpolates the trajectory as needed to detect crossings.
- When the system has symmetries, such as when several periodic orbits lie on the same line, there are ‘bad’ choices of projection line where it is impossible to resolve the order of crossings, since orbits cross at exactly the same time. Displacing the projection line a little cures this.
- If the braid is truly periodic, that is, if all the particles return to their initial configuration, then changing the projection line changes the braid, but only by *conjugation*, which does not affect the entropy [6] (Section III).

- If the trajectories are not periodic, then the method does not define a braid in the traditional sense where all the strands return to the same initial configuration. This is inconsequential to our purposes: all that matters is the order along the projection line (see also [25]). The choice of projection line changes the braid beyond simple conjugation, but this only creates an error in a small, finite number of generators, which is not important when considering long braids and does not asymptotically affect the entropy (Section III).
- If the braid is generated from chaotic trajectories, then missing a few crossings (due to, say, gaps in the data) is fine as long as the trajectories are long enough.

III. TOPOLOGICAL ENTROPY

In Section II we described how a set of trajectories in the two-dimensional dynamical system can be described as a braid in a three-dimensional space-time diagram. In this section we will describe further how this braid relates to topological information for the underlying flow.

It is worth noting that braids are not always interpreted in terms of trajectories: they arose first and are still studied as independent geometrical and algebraic objects. The reason they take center stage in the present study is through their connection to mappings of surfaces (mapping class groups). The Thurston–Nielsen theory [27, 28, 29, 30, 31] classifies mapping of surfaces according to whether they can be “deformed” to each other in a topological sense. Braids provide a convenient way of labeling the *isotopy classes* that result. So even though we will often speak here of the braid as being the primary object of interest, we are really using techniques that apply to the class of mappings labeled by a braid.

A. Entropy of a flow

Ultimately, we want to measure the topological entropy of a system directly from a braid of trajectories. Before we do this, we discuss the meaning of topological entropy of a flow or map. The topological entropy of a dynamical system measures the loss of information under the dynamics. It is closely related to the Lyapunov exponent, which measures the time-asymptotic rate of separation of neighboring trajectories. But it is in some sense a cruder quantity, since it does not require a notion of distance. A positive entropy is associated with chaos, though it tells us nothing about the size of the chaotic region. The topological entropy is an upper bound on the largest Lyapunov exponent of a flow. The two are equal only for very simple systems where stretching is uniform.

Though there are more fundamental ways to define it, we shall take our working definition of entropy to be the *asymptotic growth rate of material lines* [32]. It is fairly straightforward to measure this numerically, given a sufficiently accurate velocity field. We simply choose an initial material line and follow it for some time, interpolating new points as the line gets longer. Figure 6 shows such a line for a numerical simulation of a stirred viscous flow. Note how the exponential growth rate is very sharply defined. The topological entropy is the supremum of the growth rate over all such loops, but in practice almost any nontrivial loop (*i.e.*, that spans the domain) will grow exponentially at a rate h_{flow} .

In practical applications we often do not have access to an accurate representation of the velocity field. This is where braids come in, as a way of approximating the topological

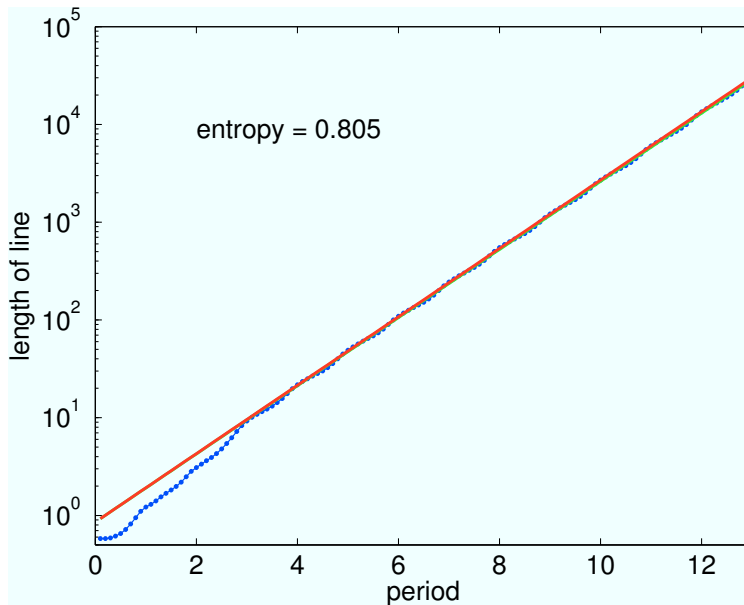


FIG. 6: The length of a material line as it is advected by a flow for many periods. The exponential growth rate is very well defined (fitted line), even though there are identical small oscillations at each period.

entropy. As we will see in Section III B, the braid provides a lower bound on the flow’s topological entropy.

B. Entropy of a braid

Figure 7 illustrates how the motion of $n = 3$ point particles can be used to put a lower bound on the topological entropy, defined here as the growth rate of material lines or loops. Here, the point particles undergo a motion described by the braid $\sigma_1\sigma_2^{-1}$. Two full periods are shown. Notice that an initial loop that is ‘caught’ on the particles is forced to follow along, since determinism implies that it cannot occupy the same point in phase space as the particles. In fact, a straightforward calculation [5] shows that for this braid the total length of the loop must grow exponentially at least at a rate $\log((3 + \sqrt{5})/2)$ per period. We call this rate the *topological entropy of the braid*, $h_{\text{braid}}^{(n)}$, to distinguish it from the true topological entropy of the flow, h_{flow} , as defined in Section III A. We have

$$h_{\text{flow}} \geq h_{\text{braid}}^{(n)} \quad (2)$$

for any braid obtained from the motion of n particles in the flow. Typically, the more particles are included in the braid, the closer $h_{\text{braid}}^{(n)}$ is to h_{flow} [14]. Note that $h_{\text{braid}}^{(1)}$ and $h_{\text{braid}}^{(2)}$ are always zero.

An essential property of $h_{\text{braid}}^{(n)}$ is that the growth *rate* of the loop is independent of specific details: for instance, if the particles are not equally spaced, or if the loop is ‘tightened’ around the particles, then the length will change, but the asymptotic growth rate will not, because all these changes amount to an additive constant in the logarithm, which gets divided by a large time.

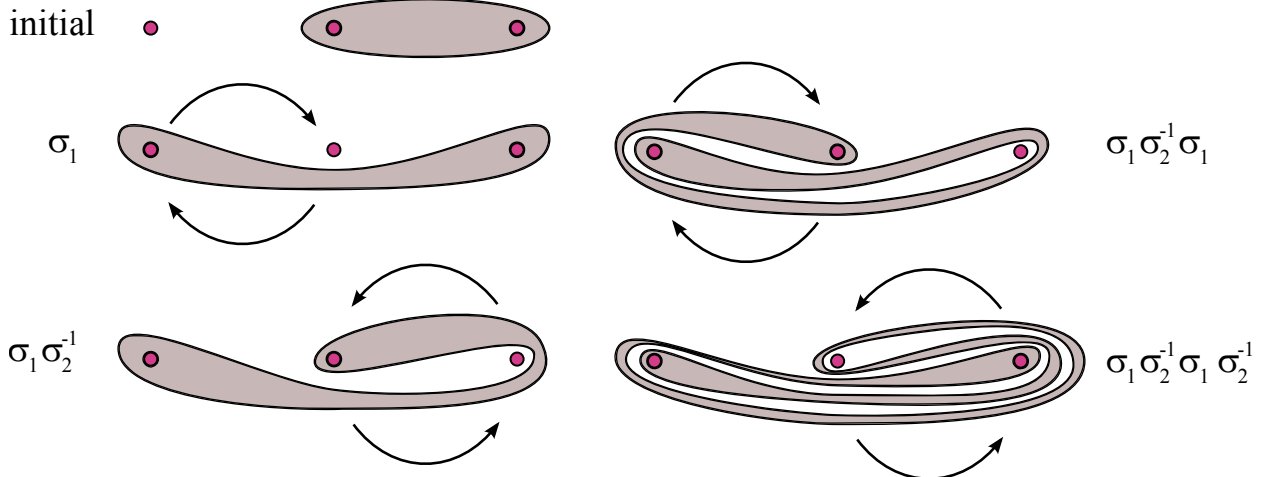


FIG. 7: For $n = 3$ particles, a loop is initially wrapped around the second and third particles. The generator σ_1 is applied, interchanging clockwise the first and second particles, followed by σ_2^{-1} , which interchanges the second and third particles counterclockwise. The loop is forced to stretch under this application. The final loop on the lower right underwent two applications of the braid $\sigma_1\sigma_2^{-1}$. If we keep applying this braid, the length of the loop will grow exponentially.

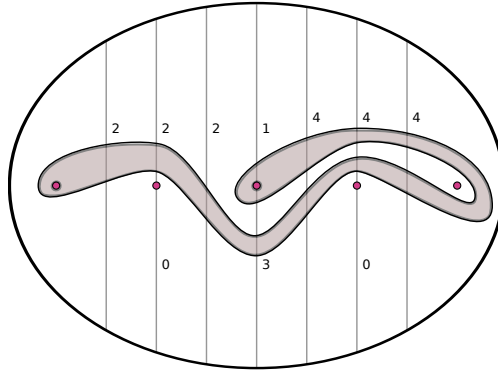


FIG. 8: A non-intersecting closed loop wrapped around $n = 5$ particles. Up to trivial deformations, the loop can be reconstructed by counting intersections with the vertical lines. In terms of the crossing numbers defined in Fig. 9, this loop has $\nu_1 = \nu_2 = 2$, $\nu_3 = \nu_4 = 4$, $\mu_1 = 2$, $\mu_3 = 1$, $\mu_5 = 4$, $\mu_2 = \mu_6 = 0$, $\mu_4 = 3$, and Dynnikov coordinate vector $\mathbf{u} = (-1, 1, -2, 0, -1, 0)$ (see Eq. (4)).

We are now faced with a task: given a sequence of generators σ_i , measured in some way or obtained numerically from a flow, what is $h_{\text{braid}}^{(n)}$? The method used in [7], based on a matrix representation of the braid group, only provides a lower bound on the braid entropy. An accurate and efficient computation has since become a lot simpler due to a new algorithm by Moussafir [33], who uses a set of coordinates to encode a loop. We describe this briefly below; for more details see [33, 34, 35]. The reader who is mostly interested in using the method can skip to the end of the section to Procedure 1.

The basic idea is simple: consider the closed loop in Fig. 8, which is wrapped around $n = 5$ particles. The loop does not intersect itself, so in two dimensions the allowable paths it can follow around the particles are far from arbitrary. The amazing fact is that we can

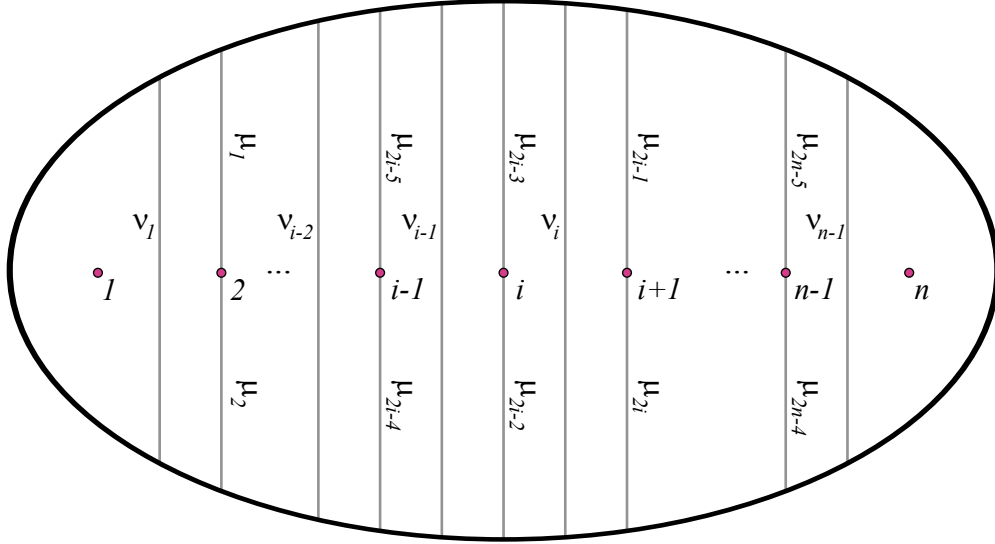


FIG. 9: Definition of the crossing numbers μ_i and ν_i . The μ_i for i odd count crossings above a particle, and below a particle for i even. The ν_i count crossings between particles.

reconstruct the entire loop, or at least the way it is threaded around the particles, by counting how many times it intersects the vertical lines in Fig. 8.

In Fig. 9 we give specific labels to the *crossing numbers*. For n particles, μ_{2i-3} (odd index) gives the number of crossings of a loop above the i th particle, and μ_{2i-2} (even index) below the same particle. The number ν_i counts the crossings between particle i and $i+1$. We have a total of $3n - 5$ crossing numbers.

This set of crossing numbers (which are all non-negative) can be reduced further: define

$$a_i = \frac{1}{2} (\mu_{2i} - \mu_{2i-1}), \quad b_i = \frac{1}{2} (\nu_i - \nu_{i+1}) \quad (3)$$

for $i = 1, \dots, n-2$. The vector of length $(2n-4)$,

$$\mathbf{u} = (a_1, \dots, a_{n-2}, b_1, \dots, b_{n-2}) \quad (4)$$

is called the *Dynnikov coordinates* of a loop. (As far as we know, this specific encoding was originally introduced by Dynnikov [34], but it is implicit in earlier work of Thurston, Dehn, and others.) The components a_i and b_i are signed integers. They can be used to exactly reconstruct the loop [35], but we shall not need to do this here. This set of coordinates is minimal: it is not possible to achieve the same reconstruction with fewer numbers.

We can also obtain the minimum number of intersections $L(\mathbf{u})$ of the loop with the horizontal line through the particles [33]:

$$L(\mathbf{u}) = |a_1| + |a_{n-2}| + \sum_{i=1}^{n-3} |a_{i+1} - a_i| + \sum_{i=0}^{n-1} |b_i|, \quad (5)$$

where b_0 and b_{n-1} can be obtained from the other coordinates as [35]

$$b_0 = - \max_{1 \leq i \leq n-2} \left(|a_i| + b_i^+ + \sum_{j=1}^{i-1} b_j \right), \quad b_{n-1} = -b_0 - \sum_{j=1}^{n-2} b_j. \quad (6)$$

The formula for $L(\mathbf{u})$ is encoded in the Matlab function `loopinter` in Appendix A 2. For example, the loop in Fig. 8 intersects the horizontal axis (the line through all the particles) 12 times. The crucial observation, which will allow a simple computation of $h_{\text{braid}}^{(n)}$, is that if the length of the loop grows exponentially, then $L(\mathbf{u})$ also grows exponentially at the same rate [27, 33].

Now that we have a way of encoding any loop, we need to find how the loop is transformed by a braid. What makes all this work is that there is a very efficient way of doing this: given a loop encoded by \mathbf{u} as in Eq. (4), each generator of the braid group σ_i simply transforms these coordinates in a predetermined manner. (Mathematically, this defines an *action* of the braid group on the set of Dynnikov coordinates.) We call these transformations the *update rules* for a generator.

The update rules are straightforward to code on a computer. (See Appendix A 2 for a Matlab implementation.) To express them succinctly,¹ first define for a quantity f the operators

$$f^+ := \max(f, 0), \quad f^- := \min(f, 0). \quad (7)$$

After we define

$$c_{i-1} = a_{i-1} - a_i - b_i^+ + b_{i-1}^-, \quad (8)$$

we can express the update rules for the σ_i acting on $\mathbf{u} = (a_1, \dots, a_{n-2}, b_1, \dots, b_{n-2})$ as

$$a'_{i-1} = a_{i-1} - b_{i-1}^+ - (b_i^+ + c_{i-1})^+, \quad (9a)$$

$$b'_{i-1} = b_i + c_{i-1}^-, \quad (9b)$$

$$a'_i = a_i - b_i^- - (b_{i-1}^- - c_{i-1})^-, \quad (9c)$$

$$b'_i = b_{i-1} - c_{i-1}^-, \quad (9d)$$

for $i = 2, \dots, n-2$. For this and the following update rules, all the other unlisted components of \mathbf{u} are unchanged under the action of σ_i or σ_i^{-1} . The leftmost ($i = 1$) and rightmost ($i = n - 1$) generators require special treatment, having update rules

$$a'_1 = -b_1 + (a_1 + b_1^+)^+, \quad (10a)$$

$$b'_1 = a_1 + b_1^+. \quad (10b)$$

for σ_1 , and

$$a'_{n-2} = -b_{n-2} + (a_{n-2} + b_{n-2}^-)^-, \quad (11a)$$

$$b'_{n-2} = a_{n-2} + b_{n-2}^-. \quad (11b)$$

for σ_{n-1} .

We need to give separate update rules for the generators σ_i^{-1} . With the definition

$$d_{i-1} = a_{i-1} - a_i + b_i^+ - b_{i-1}^-, \quad (12)$$

¹ We are using the numbering scheme of [35], but the notation of [33]. Also, we define generators σ_i as clockwise interchanges rather than counterclockwise.

the update rules for the σ_i^{-1} are

$$a'_{i-1} = a_{i-1} + b_{i-1}^+ + (b_i^+ - d_{i-1})^+, \quad (13a)$$

$$b'_{i-1} = b_i - d_{i-1}^+, \quad (13b)$$

$$a'_i = a_i + b_i^- + (b_{i-1}^- + d_{i-1})^-, \quad (13c)$$

$$b'_i = b_{i-1} + d_{i-1}^+, \quad (13d)$$

for $i = 2, \dots, n-2$. We also have

$$a'_1 = b_1 - (b_1^+ - a_1)^+, \quad (14a)$$

$$b'_1 = b_1^+ - a_1. \quad (14b)$$

for σ_1^{-1} , and

$$a'_{n-2} = b_{n-2} - (b_{n-2}^- - a_{n-2})^-, \quad (15a)$$

$$b'_{n-2} = b_{n-2}^- - a_{n-2}. \quad (15b)$$

for σ_{n-1}^{-1} .

Update rules of this form are known as *piecewise-linear*: once the mins and maxes are resolved, what is left is simply a linear operation. However, the mins and maxes are what keeps this from being a simple linear algebra problem and make the braid dynamics so rich.

Here then is a recipe for computing $h_{\text{braid}}^{(n)}$, the topological entropy of a braid of n particle trajectories:

Procedure 1 (Entropy of periodic braid)

1. Start with an arbitrary initial loop, encoded as a vector \mathbf{u} (Eq. (4)); Set m to 0;
2. For each generator in the braid, use the appropriate update rule (8)–(15) to modify \mathbf{u} ;
3. Compute the intersection number $L(\mathbf{u})$ using Eq. (5);
4. Repeat steps 2–3 for all generators in the braid;
5. Add 1 to m ; Calculate $h_{\text{braid}}^{(n)} = m^{-1} \log L(\mathbf{u})$;
6. Repeat steps 2 to 5 until $h_{\text{braid}}^{(n)}$ converges in step 5.

Remarks:

- The procedure above assumes that the braid is *periodic*, *i.e.*, is obtained from periodic orbits of the flow. In Section IV we will discuss how the method differs for random braids obtained from sampling arbitrary trajectories (which don't necessarily repeat).
- The dimension of $h_{\text{braid}}^{(n)}$ is inverse time, where the unit of time is the period over which the braid is repeated.
- Even though the discussion so far has described \mathbf{u} as a vector of integers, the initial condition for \mathbf{u} in step 1 can in practice be chosen to be a random set of real numbers. (This called a *projectivized* version of the coordinates [35].)

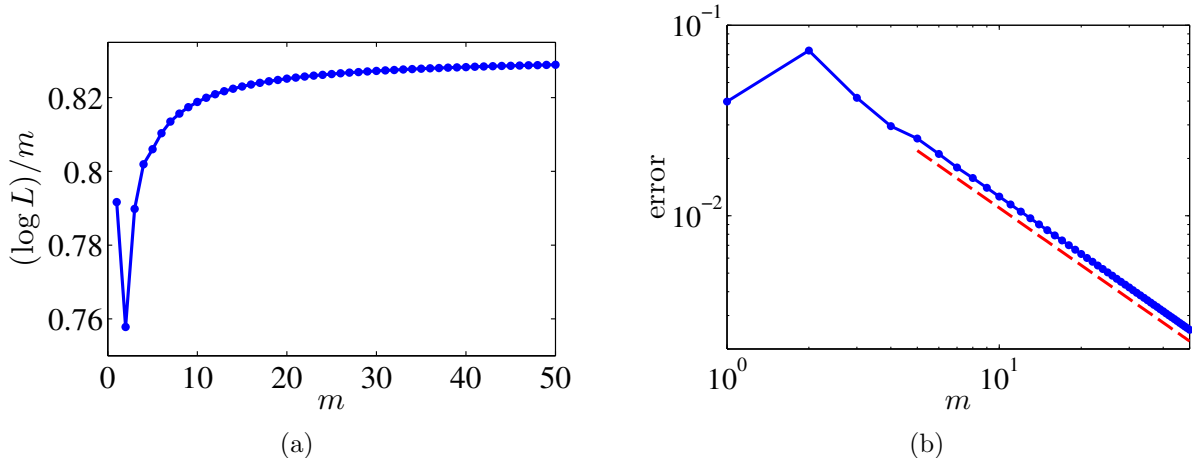


FIG. 10: For the braid $\sigma_3^{-1}\sigma_2^{-1}\sigma_3^{-1}\sigma_2\sigma_1$ in Fig. 2, (a) Entropy estimate $m^{-1} \log L(\mathbf{u})$ as a function of period m using Procedure 1. (b) Error (deviation from the true entropy $\simeq 0.83144$), showing the $1/m$ convergence (dashed line).

- As is typical of such exponential growth calculation, it is possible that the components of \mathbf{u} becomes so large that they overflow double-precision arithmetic. In that case standard ‘renormalization’ techniques can be used: divide \mathbf{u} by a large constant L_{overflow} , but keep track of how many times this division was done. Then add that multiple of $\log L_{\text{overflow}}$ to the logarithm in step 5. Another option is to use real or integer arbitrary precision arithmetic, but this slows down the calculation.
- We stress that Moussafir’s technique for the computation of a braid’s entropy is extremely rapid compared to previous methods, which typically use *train tracks* and the Bestvina–Handel algorithm [36], or combinatorial methods [26]. The rapidity arises from the fact that the algorithm keeps a bare minimum of information (the vector \mathbf{u}) to express the topology of an arbitrarily long curve. The Bestvina–Handel algorithm, however, gives more information about the braid (such as the existence of invariant curves – see Section V).

The speed of convergence of this procedure is discussed in [14, 33]. As an example, Fig. 10(a) shows the result of applying the procedure to the braid in Fig. 2, and Fig. 10(b) shows the convergence rate to the exact entropy.

IV. RANDOM BRAIDS

From the point of view of data analysis, looking at periodic braid is not general enough. Most periodic orbits in a dynamical system are unstable, and thus they cannot be detected directly. The trajectories we have access to are typically chaotic. Nevertheless, we can ask what the braid corresponding to a set of orbits tells us about a dynamical system. The answer is that its entropy approximates the ‘true’ topological entropy of the flow, and the approximation gets better as more particles are added.

There are two ways to analyze random braids generated by chaotic trajectories: without and with ensemble averaging. ‘Without averaging’ means that we have a single realization to study, say n trajectories integrated or measured up to some final time. Unless the final time is extremely long, this is not very accurate. ‘With averaging’ means that we have the luxury of repeating the experiment several times, following the same number of trajectories at each realization (assuming the flow is the same for each realization, at least in a statistical sense). We then average over the total number of realizations of the experiment, in the manner described below.

A. Entropy without averaging

Let us first describe the procedure without averaging: we assume that we have obtained a sequence of generators from the trajectories of n particles, as well as the time at which each crossing occurs (see Section II B). In the examples presented here, those trajectories were either computed from randomly-selected initial conditions, or they were obtained from measured data (the oceanic floats).

Procedure 2 (Entropy of random braid, without averaging)

1. Start with an arbitrary initial loop, encoded as a vector \mathbf{u} (Eq. (4));
2. For each generator in the braid, use the appropriate update rule (8)–(15) to modify \mathbf{u} ;
3. Compute the intersection number $L(\mathbf{u})$ using Eq. (5);
4. Plot $\log L(\mathbf{u})$ versus t , where t is a vector of times when each crossing occurs;
5. Repeat steps 2 to 4 until we can fit a line in step 4.

Remarks:

- Since the braid is random, we must keep track of the time when crossings occur.
- Most of the remarks from the periodic Procedure 1 of Section III B still apply.

Figure 11 shows an example of applying Procedure 2 to $n = 3$ particles advected by a blinking vortex flow [4, 7, 8] in the regular regime (Fig 11(a)) and chaotic regime (Fig. 11(b)). In the first case, the growth of $L(\mathbf{u})$ is roughly linear, so the entropy is zero. In the second case the growth is exponential. Note that the integration time is quite long, and in Fig. 11(b) $L(\mathbf{u})$ becomes enormous. For such long integration time, the fit for the entropy is good.

B. Entropy with averaging

To get a more accurate measurement of $h_{\text{braid}}^{(n)}$ for random braids, ensemble averaging is desirable, if we have that luxury. To implement this, we integrate a set of n trajectories N_{real} times, randomizing the initial condition for each realization. We obtain a list of $n \times N_{\text{real}}$ trajectories for times $0 \leq t \leq t_{\text{max}}$, from which we compute N_{real} braids and vectors of crossing times. To do the averaging, we need to be able to compare $L(\mathbf{u})$ at the same times for each braid, but since crossings occur at different times we cannot do this directly.

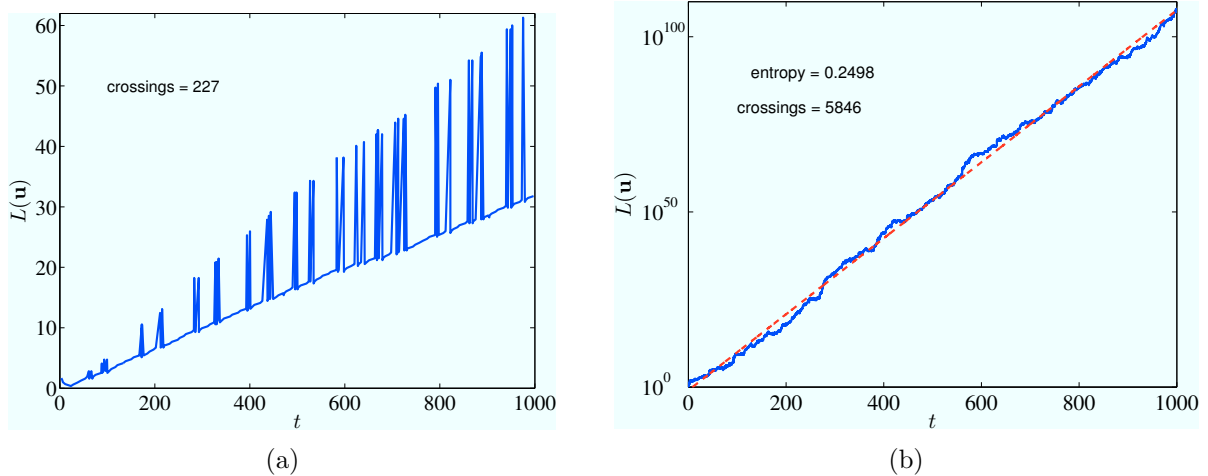


FIG. 11: (a) The number of crossings of a loop, versus time, for the blinking vortex flow in the regular regime (circulation $\Gamma = 0.5$, co-rotating vortices; see [7]). The growth of $L(\mathbf{u})$ is linear. (b) Same as in (a), but in the chaotic regime (circulation $\Gamma = 16.5$, counter-rotating vortices; see [7]). The vertical axis is now on a log scale; the slope of the line gives the braid entropy (Procedure 2).

We instead break up the total time interval into equal subintervals of length Δt , and for each subinterval and each realization we record $L(\mathbf{u})$ up to time $q\Delta t$, where q is an integer with $0 \leq q\Delta t \leq t_{\max}$. We finally obtain N_{real} lists of $[t_{\max}/\Delta t]$ (square brackets denote the integer part) intersection numbers $L(\mathbf{u})$, all sampled at the same times corresponding to each subinterval. The whole procedure is summarized as:

Procedure 3 (Entropy of random braid, with averaging)

1. Start with N_{real} lists of intersection numbers $L(\mathbf{u})$ and their crossing times, generated following Procedure 2, steps 1–3;
2. For each realization, record the intersection numbers up to fixed times $q\Delta t$, $0 \leq q\Delta t \leq t_{\max}$;
3. At each time $q\Delta t$, compute the average $\langle \log L(\mathbf{u}) \rangle$ over all N_{real} realizations;
4. Plot $\langle \log L(\mathbf{u}) \rangle$ versus $q\Delta t$, $0 \leq q\Delta t \leq t_{\max}$, and fit a line to get $h_{\text{braid}}^{(n)}$.

Remarks:

- We average $\log L(\mathbf{u})$ rather than $L(\mathbf{u})$: not only does this ensure that Procedures 2 and 3 give the same entropy, but it also leads to smaller fluctuations.
- For best results, the number of subintervals $[t_{\max}/\Delta t]$ has to be large enough to get a good fit, but small enough that there are several crossings within each subinterval of length Δt .

Figure IV B shows an example of applying Procedure 3 with $N_{\text{real}} = 50$ realization of $n = 3$ particles advected by the same blinking vortex flow as for Fig. 11(b). Notice that the fit

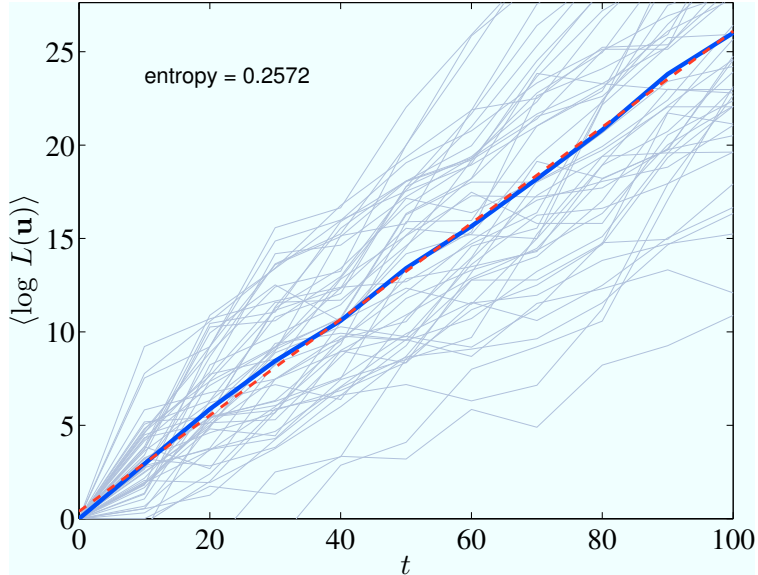


FIG. 12: Similar plot to Fig. 11(b), but after averaging $\langle \log L(\mathbf{u}) \rangle$ over $N_{\text{real}} = 50$ shorter trajectories ($t_{\text{max}} = 100$ time units rather than 1000). The average is plotted at each $\Delta t = 10$ time units (see Procedure 3). The individual trajectories are shown in the background.

is much better, even though the integration time is shorter. We used $[t_{\text{max}}/dt] = 10$ time subintervals of length $\Delta t = 10$. An explicit example in Matlab (for the Duffing oscillator) is given in Appendix A 3.

C. Oceanic floats

As a more practical application of random braids, we consider data for oceanic floats in the Labrador sea (North Atlantic) [1], discussed in the introduction (Section I A). The position of ten floats for a few months is shown in Fig. 1(a). Note that the float trajectories seem more entangled while they are confined to the Labrador sea (between Greenland and Labrador), and some eventually escape. To compute the braid, we linearly interpolate the float positions to determine when crossings occur between the $n = 10$ floats. We then use Procedure 2 to compute the entropy, as shown in Fig. 1(b), since ensemble averaging is not available here (we only have data for one experiment). We see in Fig. 1(b) that $L(\mathbf{u})$ has a convincing exponential regime for about 150 days, after which floats tend to escape the Labrador sea and $L(\mathbf{u})$ reaches a plateau. The entropy gives us a timescale for the entanglement of floats in the Labrador sea, here about $1/0.02 \simeq 50$ days. This number is easy to obtain from the raw data: there is no need for a model of the velocity field. However, the trajectories need to be long enough for a significant number of crossings to occur, and localized enough for particles to actually braid.

More context will be needed to fully understand what it means to say that the timescale for entanglement is 50 days. For instance, the method could be benchmarked by following tracers in simulations of flows comparable to the Labrador sea, in which braids can be easily computed. The measure is also useful for comparing different regions of the ocean.

Note that there has been previous work on bounding the topological entropy of experi-

mental data. Amon and Lefranc [37] have obtained lower bounds on entropy and evidence of chaotic behavior in a nonstationary optical system. See also the review by Gilmore [38].

V. DISCUSSION

There are two ways to interpret the data obtained from braids of particles. The first is to accumulate data for enough particle trajectories that a good approximation to the topological entropy h_{flow} is obtained. The drawback to this is that the convergence of $h_{\text{braid}}^{(n)}$ to h_{flow} as n gets larger appears to be fairly slow [14], though more work is needed to determine this convergence rate. In this interpretation, the braid approach is seen as a practical way of measuring h_{flow} . This interpretation is in the same spirit as a Lyapunov exponent. Its main advantage is that a single number is easy to comprehend and compare; its main drawback is that a single number doesn't capture the subtleties of a particular system.

The second interpretation is to regard $h_{\text{braid}}^{(n)}$ as the ' n -particle braiding time,' in a similar fashion that n -particle correlation functions are measured. Thus, the behavior of $h_{\text{braid}}^{(n)}$ with n carries real information, as it tells us the typical time for 3 particle trajectories to become entangled, then 4 particles, etc. We might call this the 'spectrum of braid entropies' for a dynamical system. The drawback of this approach is that it requires a more careful analysis of the data.

The method presented in this paper is limited to two-dimensional flows. Indeed, a four-dimensional braid of three-dimensional particles trajectories is not very useful, as this and all higher-dimensional braid groups are trivial (strands can always be disentangled without crossing [31]). The best alternative is to lift the trajectories of material lines to sheets in four dimensions, but this presents some daunting visualization challenges, and there is little developed theory (but see [39]).

Finally, the topological entropy $h_{\text{braid}}^{(n)}$ is only the crudest piece of information that can be extracted from a braid. Many other types of invariants can be computed [40]. However, those invariants don't necessarily have a clear interpretation in terms of dynamics. A promising avenue for obtaining much more precise information on a dynamical system is to find the isotopy class of the random braid (see Section III). This would tell us, for instance, whether some floats merely orbit each other and thus behave as one 'trajectory' from the point of view of braiding and entropy. This is akin to making a braid out of thick rope: even though each rope is made up of tiny strands, these contribute to the braid as one large strand. This sort of approach could help to identify Lagrangian coherent structures from particle trajectory data, by looking for decomposable braids. However, the tools available to do this, such as the Bestvina–Handel algorithm [36], are still slow and difficult to use on large braids. A promising approach was recently used in [35], but needs to be developed further.

Acknowledgments

The author thanks Karen Daniels, Tom Solomon, Matt Finn, Matt Harrington, and Philip Boyland for their help and comments. This work was supported by the Division of

Mathematical Sciences of the US National Science Foundation, under grant DMS-0806821.

- [1] ‘WOCE subsurface float data assembly center,’ (2004), <http://wfdac.whoi.edu>.
- [2] J. H. LaCasce, ‘Lagrangian statistics from oceanic and atmospheric observations,’ in J. B. Weiss and A. Provenzale, eds., *Transport and Mixing in Geophysical Flows, Lecture Notes in Physics*, volume 744, 165–218 (Springer, Berlin, 2008).
- [3] A. Wolf, J. B. Swift, H. L. Swinney, and J. A. Vastano, ‘Determining Lyapunov exponents from a time series,’ *Physica D* **16**, 285–317 (1985).
- [4] H. Aref, ‘Stirring by chaotic advection,’ *J. Fluid Mech.* **143**, 1–21 (1984).
- [5] P. L. Boyland, H. Aref, and M. A. Stremler, ‘Topological fluid mechanics of stirring,’ *J. Fluid Mech.* **403**, 277–304 (2000).
- [6] P. L. Boyland, M. A. Stremler, and H. Aref, ‘Topological fluid mechanics of point vortex motions,’ *Physica D* **175**, 69–95 (2003).
- [7] J.-L. Thiffeault, ‘Measuring topological chaos,’ *Phys. Rev. Lett.* **94** (8), 084502 (2005).
- [8] E. Kin and T. Sakajo, ‘Efficient topological chaos embedded in the blinking vortex system,’ *Chaos* **15** (2), 023111 (2005).
- [9] E. Gouillart, M. D. Finn, and J.-L. Thiffeault, ‘Topological mixing with ghost rods,’ *Phys. Rev. E* **73**, 036311 (2006).
- [10] J.-L. Thiffeault, M. D. Finn, E. Gouillart, and T. Hall, ‘Topology of chaotic mixing patterns,’ *Chaos* **18**, 033123 (2008).
- [11] M. D. Finn, S. M. Cox, and H. M. Byrne, ‘Topological chaos in inviscid and viscous mixers,’ *J. Fluid Mech.* **493**, 345–361 (2003).
- [12] B. J. Binder and S. M. Cox, ‘A mixer design for the pigtail braid,’ *Fluid Dyn. Res.* **49**, 34–44 (2008).
- [13] A. Vikhansky, ‘Simulation of topological chaos in laminar flows,’ *Chaos* **14** (1), 14–22 (2004).
- [14] M. D. Finn and J.-L. Thiffeault, ‘Topological entropy of braids on the torus,’ *SIAM J. Appl. Dyn. Sys.* **6**, 79–98 (2007).
- [15] M. D. Finn, J.-L. Thiffeault, and E. Gouillart, ‘Topological chaos in spatially periodic mixers,’ *Physica D* **221** (1), 92–100 (2006).
- [16] J.-L. Thiffeault and M. D. Finn, ‘Topology, braids, and mixing in fluids,’ *Phil. Trans. R. Soc. Lond. A* **364**, 3251–3266 (2006).
- [17] M. A. Stremler and J. Chen, ‘Generating topological chaos in lid-driven cavity flow,’ *Phys. Fluids* **19**, 103602 (2007).
- [18] A. Vikhansky, ‘Chaotic advection of finite-size bodies in a cavity flow,’ *Phys. Fluids* **15** (7), 1830–1836 (2003).
- [19] M. A. Berger, ‘Third order invariants of randomly braided curves,’ in H. K. Moffatt and A. Tsinobner, eds., *Topological Fluid Mechanics*, 440–448 (Cambridge University Press, Cambridge, U.K., 1990).
- [20] S. K. Nechaev, *Statistics of Knots and Entangled Random Walks* (World Scientific, Singapore; London, 1996).
- [21] E. Artin, ‘Theory of braids,’ *Ann. Math.* **48** (1), 101–126 (1947).
- [22] J. S. Birman, K. H. Ko, and S. J. Lee, ‘A new approach to the word and conjugacy problems in the braid groups,’ *Adv. Math.* **139**, 322–353 (1998).
- [23] J. S. Birman and T. E. Brendle, ‘Braids: A survey,’ in W. Menasco and M. Thistlethwaite,

- eds., *Handbook of Knot Theory* (Elsevier, Amsterdam, 2005), available at <http://arXiv.org/abs/math.GT/0409205>.
- [24] I. A. Dynnikov and B. Wiest, ‘On the complexity of braids,’ (2007), <http://arXiv.org/abs/math.GT/0403177>.
- [25] J.-M. Gambaudo and E. E. Pérou, ‘Dynamical cocycles with values in the Artin braid group,’ *Ergod. Th. Dynam. Sys.* **19**, 627–641 (1999).
- [26] M. Lefranc, ‘Alternative determinism principle for topological analysis of chaos,’ *Phys. Rev. E* **74**, 035202(R) (2006).
- [27] A. Fathi, F. Laudenbach, and V. Poénaru, ‘Travaux de Thurston sur les surfaces,’ *Astérisque* **66-67**, 1–284 (1979).
- [28] W. P. Thurston, ‘On the geometry and dynamics of diffeomorphisms of surfaces,’ *Bull. Am. Math. Soc.* **19**, 417–431 (1988).
- [29] A. J. Casson and S. A. Bleiler, *Automorphisms of surfaces after Nielsen and Thurston*, London Mathematical Society Student Texts, volume 9 (Cambridge University Press, Cambridge, 1988).
- [30] P. L. Boyland, ‘Topological methods in surface dynamics,’ *Topology Appl.* **58**, 223–298 (1994).
- [31] J. S. Birman, *Braids, Links, and Mapping Class Groups*, Annals of Mathematics Studies (Princeton University Press, Princeton, NJ, 1975).
- [32] S. E. Newhouse and T. Pignataro, ‘On the estimation of topological entropy,’ *J. Stat. Phys.* **72** (5-6), 1331–1351 (1993).
- [33] J.-O. Moussaïf, ‘On the entropy of braids,’ *Func. Anal. and Other Math.* **1** (1), 43–54 (2006).
- [34] I. A. Dynnikov, ‘On a Yang–Baxter map and the Dehornoy ordering,’ *Russian Math. Surveys* **57** (3), 592–594 (2002).
- [35] T. Hall and S. Ö. Yurttaş, ‘On the topological entropy of families of braids,’ *Topology Appl.* **156** (8), 1554–1564 (2009).
- [36] M. Bestvina and M. Handel, ‘Train-tracks for surface homeomorphisms,’ *Topology* **34** (1), 109–140 (1995).
- [37] A. Amon and M. Lefranc, ‘Topological signature of deterministic chaos in short nonstationary signals from an optical parametric oscillator,’ *Phys. Rev. Lett.* **92** (9), 094101 (2004).
- [38] R. Gilmore, ‘Topological analysis of chaotic dynamical systems,’ *Rev. Mod. Phys.* **70** (4), 1455–1529 (1998).
- [39] S. Kamada, *Braid and Knot Theory in Dimension Four*, Mathematical Surveys & Monographs (American Mathematical Society, 2002).
- [40] M. A. Berger, ‘Topological invariants in braid theory,’ *Lett. Math. Phys.* **55** (3), 181–192 (2001).

APPENDIX A: MATLAB EXAMPLE PROGRAMS

These Matlab programs can be obtained by downloading the source of this paper at <http://arXiv.org/abs/0906.3647>.

1. `gencross` and `intercross`

The function `gencross` computes the generators and crossing times for particle trajectories (see Section IIB). The function `intercross` is a helper function to `gencross` that

interpolates crossings. Both these functions are simple implementations with few bells and whistles: `gencross` deals with two or three adjacent particles crossing between successive timesteps, but it does not attempt to refine the trajectory (by interpolation or integration) to resolve crossings. If it gets confused because too many crossings are occurring between two successive timesteps, there is not other option but to refine the data further.

```
function [varargout] = gencross(t,X,Y)
%GENCROSS Find braid generators from crossings of trajectories.
% G = GENCROSS(T,X,Y) finds the braid group generators associated with
% crossings of particle trajectories. Here T is a column vector of times,
% and X and Y are coordinates of particles at those times. X and Y have
% the same number of rows as T, and N columns, where N is the number of
% particles. A projection on the X axis is used to define crossings.
%
% [G,TC] = GENCROSS(T,X,Y) also returns a vector of times TC when the
% crossings occurred.

% Find the permutation at each time.
[Xperm,Iperm] = sort(X,2);
dperm = diff(Iperm,1); % Crossings occur when the permutation changes.
icr = find(any(dperm,2)); % Index of crossings.
gen = []; tcr = [];

for i = 1:length(icr)
% Order (from left to right) of particles involved in crossing.
igen = find(dperm(icr(i),:));
j = 1;
while j < length(igen)
if ~sum(dperm(icr(i),igen(j:j+1)))
%
% Crossing involves a pair of particles.
%
p = Iperm(icr(i),igen(j:j+1)); % The two particles involved in crossing.
[tt,dY] = interpcross(t,X,Y,icr(i),p(1),p(2));
tcr = [tcr;tt]; gen = [gen; igen(j)*dY];
j = j+2;

elseif ~sum(dperm(icr(i),igen(j:j+2)))
%
% Crossing involves a triplet of particles.
% Two cases are possible:
%
if Iperm(icr(i),igen(j)) == Iperm(icr(i)+1,igen(j)+1)
% Case 1: ABC -> CAB

% Particles B&C cross first
p = Iperm(icr(i),igen([j+1 j+2]));
[tt,dY] = interpcross(t,X,Y,icr(i),p(1),p(2));
tcr = [tcr;tt]; gen = [gen; igen(j+1)*dY];

% Particles A&C cross second
p = Iperm(icr(i),igen([j j+2]));
[tt,dY] = interpcross(t,X,Y,icr(i),p(1),p(2));
tcr = [tcr;tt]; gen = [gen; igen(j)*dY];
elseif Iperm(icr(i),igen(j)) == Iperm(icr(i)+1,igen(j)+2)
% Case 2: ABC -> BCA

% Particles A&B cross first
p = Iperm(icr(i),igen([j j+1]));
[tt,dY] = interpcross(t,X,Y,icr(i),p(1),p(2));
tcr = [tcr;tt]; gen = [gen; igen(j)*dY];

% Particles A&C cross second
p = Iperm(icr(i),igen([j j+2]));
[tt,dY] = interpcross(t,X,Y,icr(i),p(1),p(2));
tcr = [tcr;tt]; gen = [gen; igen(j+1)*dY];
else
```

```

        error('something''s wrong with triple crossing -- increase resolution')
    end
    j = j+3;
else
    error('too many simultaneous crossings -- increase resolution')
end
end
end
varargout{1} = gen;
if nargout > 1, varargout{2} = tcr; end

```

```

function [tc,dY] = interpcross(t,X,Y,itc,p1,p2)
%INTERPCROSS Interpolate a crossing.
% [TC,DY] = INTERPCROSS(T,X,Y,ITC,P1,P2) is a helper function for
% GENCROSS. The input is the data T,X,Y (described in the help for
% GENCROSS); the index ITC of the time of crossing (i.e., the particles
% cross between T(ITC) and T(ITC+1); and the indices P1 and P2 of the two
% particles that are crossing. INTERPCROSS returns the interpolated
% crossing time TC, as well as DY (the sign of the difference in Y
% coordinates) which determines the sign of the generator.

% Refine crossing time and position (linear interpolation).
dt = t(itc+1) - t(itc); % Time interval.
% Particle velocities in that interval.
U1 = (X(itc+1,p1) - X(itc,p1)) / dt;
V1 = (Y(itc+1,p1) - Y(itc,p1)) / dt;
U2 = (X(itc+1,p2) - X(itc,p2)) / dt;
V2 = (Y(itc+1,p2) - Y(itc,p2)) / dt;
% Interpolated crossing time and Y coordinates.
dtc = -(X(itc,p2) - X(itc,p1)) / (U2-U1);
tc = t(itc) + dtc;
Y1c = Y(itc,p1) + dtc*V1;
Y2c = Y(itc,p2) + dtc*V2;
dY = sign(Y1c-Y2c);
% The sign of Y1c-Y2c determines if the crossing is g or g^-1.
if dY == 0,
    error('can''t resolve sign of generator -- increase resolution');
end
end

```

2. loopsigma and loopinter

The function `loopsigma` applies a sequence of braid group generators to a loop (Section III B, Eqs. (8)–(15)). The function `loopinter` computes $L(\mathbf{u})$, the minimum number of intersections of a loop with the horizontal axis (Section III B, Eq. (5)).

```

function up = loopsigma(ii,u)
%LOOPSIGMA Act on a loop with a braid group generator sigma.
% UP = LOOPSIGMA(J,U) acts on the loop U (encoded in Dynnikov coordinates)
% with the braid generator sigma_J, and returns the new loop UP. J can be
% a positive or negative integer (inverse generator), and can be specified
% as a vector, in which case all the generators are applied to the loop
% sequentially from left to right.

n = length(u)/2 + 2;
a = u(1:n-2); b = u((n-1):end);
ap = a; bp = b;
pos = @(x)max(x,0); neg = @(x)min(x,0);
for j = 1:length(ii)
    i = abs(ii(j));
    if ii(j) > 0
        switch(i)
            case 1
                bp(1) = a(1) + pos(b(1));

```

```

    ap(1) = -b(1) + pos(bp(1));
case n-1
    bp(n-2) = a(n-2) + neg(b(n-2));
    ap(n-2) = -b(n-2) + neg(bp(n-2));
otherwise
    c = a(i-1) - a(i) - pos(b(i)) + neg(b(i-1));
    ap(i-1) = a(i-1) - pos(b(i-1)) - pos(pos(b(i)) + c);
    bp(i-1) = b(i) + neg(c);
    ap(i) = a(i) - neg(b(i)) - neg(neg(b(i-1)) - c);
    bp(i) = b(i-1) - neg(c);
end
elseif ii(j) < 0
    switch(i)
    case 1
        bp(1) = -a(1) + pos(b(1));
        ap(1) = b(1) - pos(bp(1));
    case n-1
        bp(n-2) = -a(n-2) + neg(b(n-2));
        ap(n-2) = b(n-2) - neg(bp(n-2));
    otherwise
        d = a(i-1) - a(i) + pos(b(i)) - neg(b(i-1));
        ap(i-1) = a(i-1) + pos(b(i-1)) + pos(pos(b(i)) - d);
        bp(i-1) = b(i) - pos(d);
        ap(i) = a(i) + neg(b(i)) + neg(neg(b(i-1)) + d);
        bp(i) = b(i-1) + pos(d);
    end
end
a = ap; b = bp;
end
up = [ap bp];

```

```

function int = loopinter(u)
%LOOPINTER The number of intersections of a loop with the real axis.
% I = LOOPINTER(U) computes the minimum number of intersections of a loop
% (encoded in Dynnikov coordinates) with the real axis. (See Moussafir
% (2006), Proposition 4.4.) U is either a row-vector, or a matrix of
% row-vectors, in which case the function acts vectorially on each row.

n = size(u,2)/2 + 2;
a = u(:,1:n-2); b = u(:,(n-1):end);
cumb = [zeros(size(u,1),1) cumsum(b,2)];
% The number of intersections before/after the first and last punctures.
% See Hall & Yurttas (2009).
b0 = -max(abs(a) + max(b,0) + cumb(:,1:end-1),[],2); bn = -b0 - sum(b,2);
int = sum(abs(b),2) + sum(abs(a(:,2:end)-a(:,1:end-1)),2) ...
    + abs(a(:,1)) + abs(a(:,end)) + abs(b0) + abs(bn);

```

3. proc3_example

The function `proc3_example` computes $L(\mathbf{u})$ for a random braid of 4 particles advected by the Duffing oscillator, using averaging over 100 realizations (see Section IV, Procedure 3).

```

function proc3_example

% Procedure 3 example:
% 4 particles advected by the Duffing oscillator, average over realizations.
n = 4; Nreal = 100;
tmax = 100; dt = 10; npts = 3000;
X = zeros(npts,n); Y = zeros(npts,n);
Ll = zeros(Nreal,tmax/dt); tl = dt*(1:tmax/dt);
rand('twister',2);
for r = 1:Nreal
    fprintf(1,'Realization %d\n',r)

```

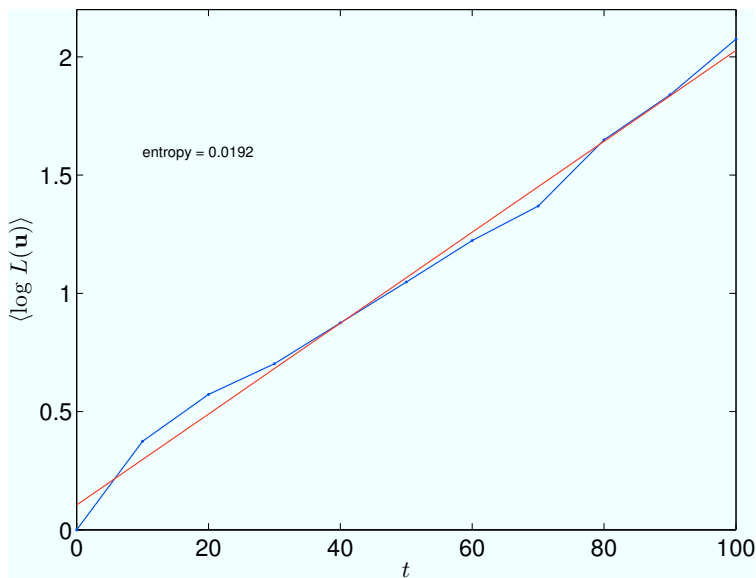


FIG. 13: Output of proc3_example (Section A 3).

```

% Compute n particle trajectories, from random initial conditions.
for i = 1:n
    [t,xy] = ode45(@duffing,linspace(0,tmax,npts)',4*rand(1,2)-2);
    X(:,i) = xy(:,1); Y(:,i) = xy(:,2);
end
[gen,tc] = gencross(t,X,Y); % Find generators and crossing times.
% Act with the generators on a random initial loop.
up = rand(1,2*(n-2)); up = up/loopinter(up);
for i = 1:length(gen), up = [up;loopsigma(gen(i),up(end,:))]; end
% Find the number of intersections with the real axis.
L{r} = loopinter(up);
% Keep intersections at a list of fixed time intervals dt, for averaging.
for q = 1:(tmax/dt)
    idx = find(tc <= t1(q));
    Ll(r,q) = L{r}(idx(end));
end
end
logLavg = [0 mean(log(Ll),1)]; t1 = [0 t1];
m = polyfit(t1,logLavg,1); % Fit a line
figure(2), plot(t1,logLavg,'b.-'), hold on
text(10,1.6,sprintf('entropy = %.4f',m(1)))
plot(t1,m(1)*t1+m(2),'r-'), hold off
xlabel('t'), ylabel('<math>\langle \log L \rangle</math>')

% -----
function yt = duffing(t,y)

delta = 1; gamma = 4; omega = 2;
yt = zeros(size(y));
yt(1,:) = y(2,:);
yt(2,:) = y(1,:).*(1 - y(1,:).*y(1,:)) + gamma*cos(omega*t) - delta*y(2,:);

```